OPEN

The Role of Magnetic Resonance Imaging in (Future) Cancer Staging
Note the Nodes

Tom W.J. Scheenen, PhD*† and Patrik Zamecnik, MD*

Abstract: The presence or absence of lymph node metastases is a very important prognostic factor in patients with solid tumors. Current invasive and noninvasive diagnostic methods for N-staging like lymph node dissection, morphologic computed tomography/magnetic resonance imaging (MRI), or positron emission tomography–computed tomography have significant limitations because of technical, biological, or anatomical reasons. Therefore, there is a great clinical need for more precise, reliable, and noninvasive N-staging in patients with solid tumors. Using ultrasmall superparamagnetic particles of ironoxide (USPIO)-enhanced MRI offers noninvasive diagnostic possibilities for N-staging of different types of cancer, including the 4 examples given in this work (head and neck cancer, esophageal cancer, rectal cancer, and prostate cancer). The excellent soft tissue contrast of MRI and an USPIO-based differentiation of metastatic versus nonmetastatic lymph nodes can enable more precise therapy and, therefore, fewer side effects, essentially in cancer patients in oligometastatic disease stage. By discussing 3 important questions in this article, we explain why lymph node staging is so important, why the timing for more accurate N-staging is right, and how it can be done with MRI. We illustrate this with the newest developments in magnetic resonance methodology enabling the use of USPIO-enhanced MRI at ultrahigh magnetic field strength and in moving parts of the body like upper abdomen or mediastinum. For prostate cancer, a comparison with radionuclide tracers connected to prostate specific membrane antigen is made. Under consideration also is the use of MRI for improvement of ex vivo cancer diagnostics. Further scientific and clinical development is needed to assess the accuracy of USPIO-enhanced MRI of detecting small metastatic deposits for different cancer types in different anatomical locations and to broaden the indications for the use of (USPIO-enhanced) MRI in lymph node imaging in clinical practice.

Key Words: cancer, MRI, USPIO, lymph nodes, N-stage, contrast agent, lymphography

(*Invest Radiol* 2021;56: 42–49)

WHY ARE LYMPH NODES IMPORTANT FOR ONCOLOGIC STAGING?

In oncology, the TNM classification system is used as a standard for staging of malignant tumors, in which the T describes the size of the primary tumor and its relation to the surrounding tissue, the N indicates the involvement of regional lymph nodes, and the M describes distant metastases. Many primary solid malignancies metastasize to the lymph nodes first, which marks a crucial step in tumor progression. From this step on, local tumor treatment of only the primary tumor is no longer sufficient to cure the patient. Nodal involvement often marks the difference between treatment with curative intent and palliative therapies.

Therefore, an accurate oncologic staging (N-staging) of lymph nodes is of utmost importance for therapy planning. Based on the localization of the tumor and its possibilities of lymphatic spread, there are several possibilities for N-staging. Historically, the oldest method is surgical removal of the lymph node: a lymph node dissection with subsequent histopathological evaluation. However, current clinical experience shows significant problems and diagnostic insufficiencies of this method, for which we will give a couple of examples.

In head and neck cancer patients, the prevalence of occult nodal metastases in clinically negative (cN0) head and neck cancer patients exceeds 20%.[1] This is why the cervical lymphatic nodes are resected rather extensively to eradicate subclinical tumor deposits. As a consequence, many truly node negative patients undergo unnecessary surgery or adjuvant radiotherapy of the neck and suffer from the associated early- and long-term morbidity.[2–5]

In esophageal cancer, the standard of care in curative treatment is neoadjuvant chemoradiotherapy (nCRT) and subsequent surgical resection of the primary tumor with locoregional lymph nodes.[6] The accuracy to detect locoregional lymph node metastases after nCRT is only low to moderate with positron emission tomography (PET)–computed tomography (CT) or endoscopic ultrasound.[7] With on average only 31% to 38% of patients who have lymph node metastases after nCRT,[6] the international guidelines still recommend lymph node dissection in all patients,[8,9] resulting in overtreatment of this patient population.

In rectal cancer, diagnostic lymph node staging is still a major challenge,[10–12] and the presence of lymph node metastases is a key factor determining treatment regimens and prognosis.[13] Lymph nodes at risk of metastasis in rectal cancer are located in the mesorectum and often smaller than 5 mm[14,15] but are difficult to reliably assess on the basis of size and shape, especially after neoadjuvant chemoradiation.[16,17] Therefore, the standard treatment is a total mesorectal resection, in which the rectal tumor and (large part of) the mesorectum including lymph nodes are completely removed.

Nodal status in prostate cancer is also of high significance for disease prognosis and choice of treatment. The current gold standard for assessing this still is an invasive (extended-) pelvic lymph node dissection,[18] associated with a considerable complication rate.[19] With the procedure, lymph nodes are harvested in a predefined dissection field, but nodes outside this field are missed (eg, in pararectal and internal iliac area).[20–22] In addition, small nodes (<3–4 mm) within the dissection area can also be missed during the surgery, so altogether the procedure can lead not only to an underestimation but also to a false-negative diagnosis of lymph node involvement.[20] For lymph node–negative patients, the removal of—retrospectively healthy—nodes is of no benefit to the patient and puts him at risk for complications of the diagnostic procedure. The benefit for cancer outcome of removing metastatic lymph nodes in prostate cancer is under intense debate. In a recent study[23] describing the long-term outcomes of prostate cancer patients

after a salvage lymph node dissection, the authors came to conclusion that, in contrast with previous evidence, most patients recurred after salvage lymph node dissection and eventually died of prostate cancer. These results underline once more an urgent need for new effective diagnostic and subsequent therapeutic methods for lymph node metastases.

Noninvasive alternatives for nodal dissections as a tool for N-staging are magnetic resonance imaging (MRI) or CT, which usually depend on the evaluation of nodal size and shape as criteria for metastatic involvement. With (partial) metastases present also in small nodes, and benign nodes that enlarge due to, for example, inflammation, the performance to differentiate between benign and malignant nodes using morphologic criteria is poor (see, eg, Refs.[16,24]). Whereas diffusion weighted imaging plays a dominant role in the multiparametric MRI assessment of localized prostate cancer,[25,26] in metastatic lymph node detection and differentiation, its role is controversial. The use of diffusion weighted imaging in lymph node evaluation is partially reported as highly effective, but a recent meta-analysis shows low sensitivity down to 41%,[27] particularly in prostate cancer patients. Therefore, the need for more specific and sensitive reliable imaging methods for N-staging using MRI is obvious. At the moment, the most effective solution to this problem is MRI enhanced with the aid of ultrasmall superparamagnetic particles of ironoxide (USPIO). Over the last years, many different USPIOs were tested for different applications.[28] However, to our knowledge, only 2 substances were evaluated on patients in phase II and III studies with larger patient numbers and were considered for oncologic lymph node imaging: ferumoxtran-10 and ferumoxytol.

Ferumoxytol (Feraheme; AMAG Pharmaceuticals, Waltham, MA) was tested in several studies to evaluate its lymphotropic properties in oncologic imaging. A recent phase II study describing experience with 39 patients with prostate, bladder and kidney cancer showed sensitivity and specificity of 98.0%, and 64.4%, respectively, using a dosage of 7.5 mg Fe/kg body weight. However, the authors concluded that although ferumoxytol-enhanced magnetic resonance (MR) lymphography can be useful in settings without an available targeted PET agent, issues of iron overload and repeatability of ferumoxytol-enhanced MR lymphography remain concerns for this method.[29] Moreover, in 2015 the Food and Drug Administration issued a black box warning regarding ferumoxytol[30] significantly restricting the indications and off-label use of ferumoxytol because of potentially life-threatening allergic reactions. This led partially to termination of already running promising studies.[31]

Ferumoxtran-10 (Ferrotran; SPL Medical BV, Nijmegen, the Netherlands) showed in several patient studies high lymphotropic behavior at a low dosage of 2.6 mg Fe/kg body weight[33,34] and has been reintroduced in clinical research and clinical care.[32] It is available for clinical studies and on terms of Named Patient Use Programs in the Netherlands and in Switzerland, and a large phase III international (the Netherlands, Switzerland, and Germany) multicenter pivotal trial has recently started. Ferumoxtran-10 nanoparticles, administered intravenously 24 to 36 hours before MRI, accumulate in macrophages and in healthy lymphatic tissue. The presence of paramagnetic iron oxide particles locally disturbs the magnetic field homogeneity, causing MR signal loss on T2*-weighted imaging. On the contrary, suspicious lymph
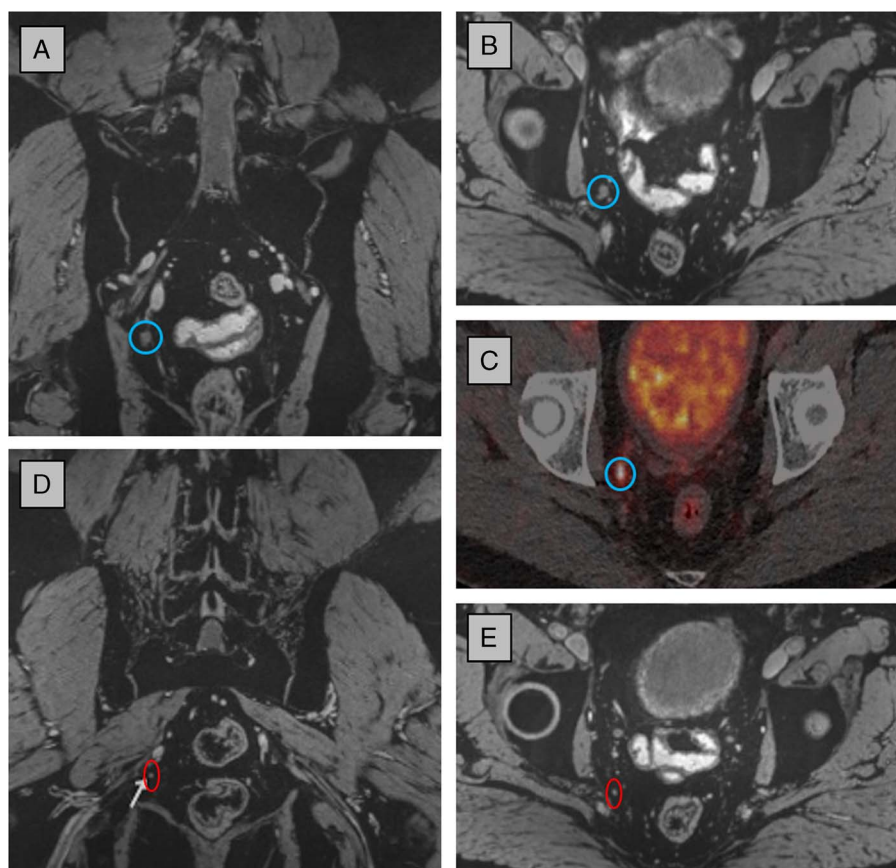
FIGURE 1. USPIO-enhanced MRI at 3 T and ^{68}Ga-PSMA PET-CT of a patient with recurrent prostate cancer (PSA level, 3.9 ng/mL). A large (7 mm) metastatic lymph node was visible on both modalities: blue circle in coronal (A) and axial image (B) and in fused PSMA PET-CT (C). Posterior to this node, one of multiple smaller metastatic nodes (2–3 mm) is indicated with a red circle in a coronal (D) and axial (E) view of the 3D MRI data set, which was not visible on PSMA PET-CT. Part of image and legend adapted from Fortuin et al.[32] Magnetic resonance imaging parameters: 3-dimensional T2*-weighted MRI with echo time 12 milliseconds (2 combined echoes), resolution 0.85 × 0.85 × 0.85 mm, acquisition time 10 hours 10 minutes.

nodes without accumulation of nanoparticles, retain a high MR signal (example in Fig. 1, from Fortuin et al[32]). Wu et al[35] analyzed earlier studies with ferumoxtran-10 and reported sensitivities up to 90% and specificities up to 96% for nodal involvement in several types of cancer.

Besides MRI, for staging of prostate cancer patients, radionuclide tracers (eg [68]Gallium or [18]Fluorine) attached to prostate-specific membrane antigen (PSMA) have been introduced in clinical studies in the last years. These are examples of targeted imaging biomarkers for the identification of prostate cancer metastases. Their relative ease of clinical adoption illustrates again the great need for a noninvasive assessment of nodal (and bone) metastatic involvement. Prostate-specific membrane antigen is a cell-surface glycoprotein, which is overexpressed on most PCa cells.[36,37] The published data regarding the sensitivity and specificity are, however, inconsistent. In a large meta-analysis,[38] pooled sensitivity for lymph node involvement of 75% and pooled specificity of 99% were reported for primary staging; a recent prospective trial by Hofman et al[39] demonstrated a (patient-based) sensitivity and specificity of 0.85 and 0.98, respectively, for the detection of both metastatic lymph nodes as well as distant metastases with ^{68}Ga-PSMA PET-CT. These authors specifically identified difficulties (sampling errors, missed nodes) in using histopathology of resected nodes as ground truth, so they reported their numbers on patient level rather than on nodal level and incorporated 6-month follow-up with repeated imaging for validation. Contrary to these high values, other recent data show low sensitivities of PSMA PET-CT in the detection of lymph node metastases of 42%,[40] 41% (SALT trial),[41] and 31%[42] at high specificities of 91%, 94%, and 97% respectively. In these studies, the median size of missed metastases was 3 mm or less, significantly smaller than the median size of detected metastases (exemplified in Fig. 1, from Fortuin et al[32]).

WHY ARE NODES NOW MORE IMPORTANT THAN EVER BEFORE?

As described above, many different types of solid cancers have a high propensity to metastasize first to locoregional and distant lymph nodes. The possibilities to selectively treat individual metastatic deposits with image-guided surgery, focal ablations and radiotherapy are continuously improving. In this context, the newest developments in the field of radiotherapy are of special interest: MR-guided radiotherapy. Guidance of early (nodal) metastatic disease with USPIO–enhanced MRI can be used for MR-guided radiotherapy with an MR linear accelerator. Under direct MRI guidance in a combined system, boundaries of the therapeutic target volume defined in a pretreatment MRI examination can be made strict and more accurate using the excellent soft tissue contrast of MRI. In addition, the hypofractionation of radiotherapy can treat small volumes with high doses in fewer visits.[43] The combination of these technical possibilities will lead to a more precise and individualized treatment with less side effects and (taking into consideration a growing number of hardware installations worldwide) better availability of this kind of treatment for more patients with (first of all oligometastatic) lymphatic spread. It could postpone or even prevent systemic treatment, which can improve disease management in different types of cancer.

Next to this, increased certainty of the absence of lymph node metastases is of equal importance. Current clinical practice often
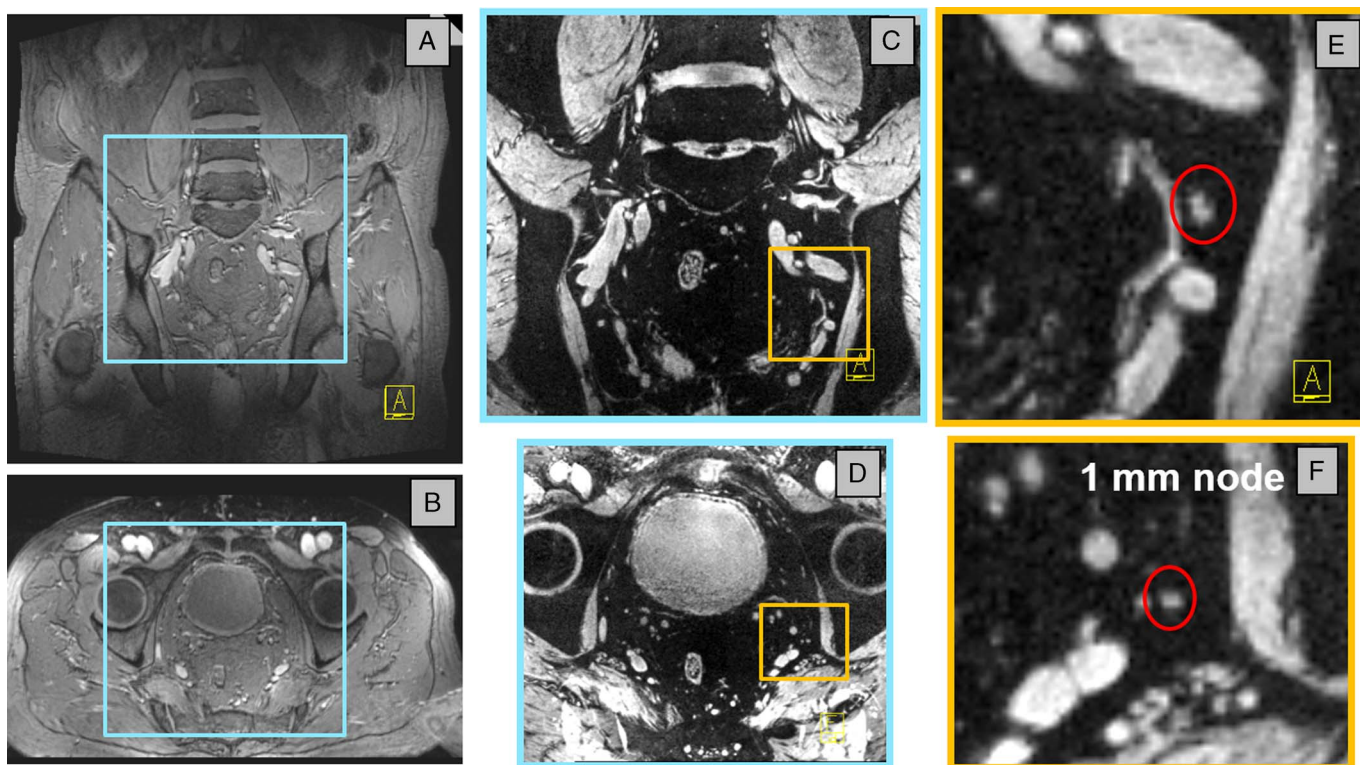

FIGURE 2. USPIO-enhanced MRI of a 71-year-old patient (94 kg) with metastasized prostate cancer, measured at 7 T, 28 hours after particle administration. Magnetic resonance imaging was performed with an 8-channel transmit/receive coil at 1 echo time with the time interleaved acquisition of mode technique homogenizing image contrast. A coronal (A) and axial (B) overview shows the patients anatomy, whereas the USPIO-enhanced images are iron-sensitive (C and D decreased FOV from blue boxes in A and B). Zooming in on the iron-sensitive MRI reveals a tiny white spherical structure: a 1-mm short axis metastasized lymph node in the red circle (E and F enlargement of yellow boxes in C and D). Parameters: 3D T2*-weighted MRI with echo time 8 milliseconds, resolution 0.66 × 0.66 × 0.66 mm, acquisition time 10 minutes.

employs considerable overtreatment for precautionary reasons. Knowledge of absence of nodal invasion in the individual patient would fit in trends toward safely minimizing treatment, reducing overtreatment, and decreasing treatment-related comorbidities. Either way, highly sensitive detection of small lymph node metastases is urgently needed. If realized, it can be possible to catch the disease at an early stage of metastatic involvement, so-called oligometastatic disease (eg, in prostate cancer[44–46]). If lymphatic spread has only just begun, an early and accurate, targeted, image-guided focal treatment of the first metastases could delay the course of the disease, or perhaps even still cure the patient.

HOW CAN WE VISUALIZE NODES IN VIVO WITH MRI?

With superb soft-tissue contrast, MRI is able to visualize lymph nodes within lipid tissue by anatomical/morphological means. Either lipid suppression or water excitation can be used to increase contrast between the lymph nodes and surrounding lipid tissue. However, as mentioned above, the morphological criteria cannot safely differentiate between metastatic and nonmetastatic lymph nodes. Only by using a functional MRI contrast like ferumoxtran-10, one can discriminate between normal lymphatic tissue that has taken up USPIO nanoparticles and metastatic lymph nodes or metastatic deposits within the lymph nodes (partial metastases) that have not taken up the particles and retain high MRI signal on T2*-weighted MRI pulse sequences. Whereas in the early 2000s, USPIO-enhanced MRI was acquired in 2-dimensional multislice series with inherent pencil-like dimensions of voxels (eg, $0.56 \times 0.56 \times 3.00$ mm at 1.5 T and $0.50 \times 0.50 \times 2.50$ mm at 3.0 T),[47] imaging technology has improved and 3-dimensional (3D) T2*-weighted acquisitions can now be acquired routinely at 3 T at sub-millimeter isotropic resolution (eg, 0.85 mm isotropic), visualizing lymph nodes of sizes down to 2 mm. When using ultra-high field strength and different adaptations to mitigate the challenges for large field-of-view body imaging at 7 T,[48,49] even suspicious lymph nodes with a short-axis size of 1 mm can be visualized (Fig. 2).

When acquiring multiple gradient echoes in the water-excited scan, the signal decay of the lymph nodes can be quantified with its corresponding T2* relaxation time, and images can be computed at different echo times using all gradient echo signals.[50] If this is performed in patients after infusion of nanoparticles, the differences in signal behavior of lymph nodes with and without USPIO accumulation can be exploited in reconstructions of multiple images at different echo times (Fig. 3). At 7 T, separate scans with either water or lipid (with partial water) excitation provide an anatomical overview of the body region at hand as well as the iron-sensitive signal intensity, reconstructed at a chosen echo time, discriminating between nodes with and without USPIO accumulation[51] (supplementary materials, http://links.lww.com/RLI/A584: movie from a patient with rectal cancer [rectum 7T 4 nodes]).

LYMPH NODES IN MOTION

The detection of suspicious lymph nodes from, for example, esophageal or pancreatic cancer requires additional efforts. Artifacts from respiratory and cardiac motion can easily obscure signal from small structures in the upper abdomen and mediastinum.[52] Traditionally, MRI in the upper abdomen is performed with repeated breathhold instructions for the patient in a limited number of slices in each breathhold. In the ideal situation of absence of breathing in prolonged apnea, mediastinal and upper abdominal lymph nodes down to 2 mm in size could be visualized with USPIO-enhanced MRI at 3 T,[53] but this is prohibited to settings with an MR system in the operating room. Three-dimensional MRIs of larger field of views are limited in spatial resolution by the allowed measurement time of breathhold scans (~18 seconds), so different pulse sequences and k-space sampling schemes for motion mitigation in the thorax and upper abdomen have been proposed for free-breathing motion-compensated MRI.[54–56] T2* weighting for USPIO-enhanced MRI is achieved by gradient echo imaging. If this is combined with the newer pulse sampling schemes, functional contrast in small lymph
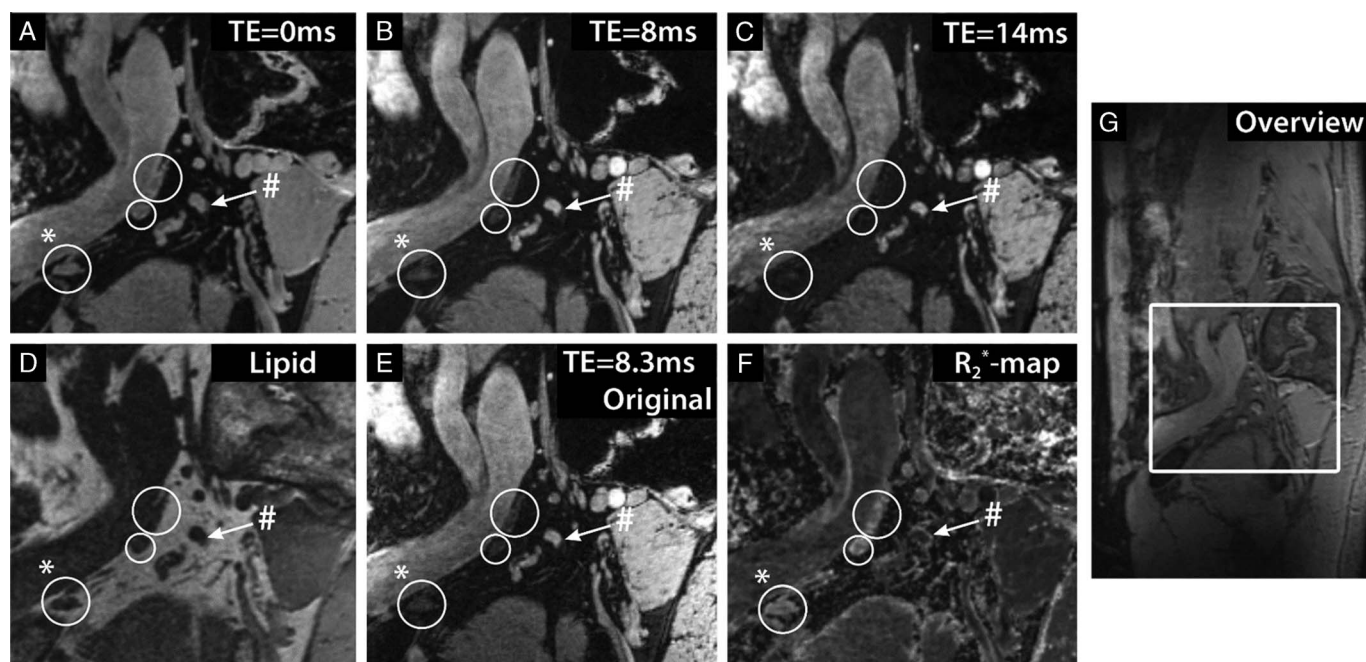

FIGURE 3. The effect of USPIOs at 7 T in the lymph nodes of a 54-year old patient with prostate cancer. A sagittal image is shown at different computed echo times (TEs) (A–C), lipid selective imaging (D), and the original multigradient echo water-selective imaging at TE 8.3 milliseconds (E). In addition, a map of fitted R_2^* relaxation rates is depicted (F). Three lymph nodes accumulated USPIO particles and rapidly lost MR signal intensity with increasing TE (white circles) and 1 suspicious lymph node without USPIOs retained MR signal intensity with TE (white arrow). A sagittal overview image is also shown (G). The lymph node marked with (#) showed a slow signal decay, with a low R_2^* value of 80 ± 6 s^{-1}, whereas the lymph node marked with (*) showed a fast R_2^* decay, with a high R_2^* value of 247 ± 25 s^{-1}. A small fatty hilus can be seen in the node marked with (*). Figure adapted from Philips et al.[51]
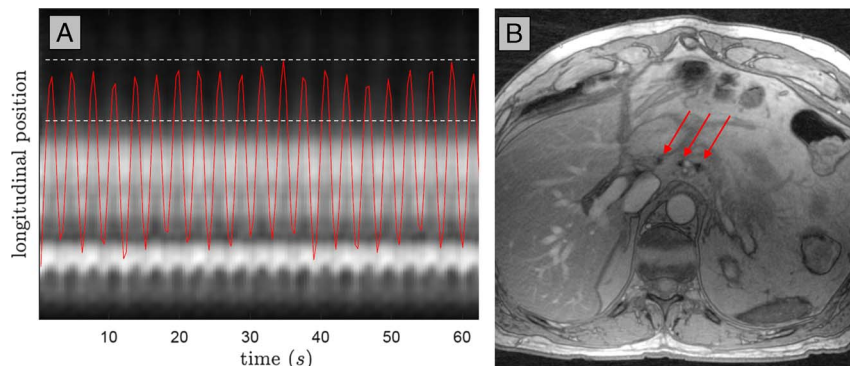
FIGURE 4. Motion-compensated USPIO-enhanced MRI at 3 T of the upper abdomen of a patient with esophageal cancer. During continuous breathing radial k-space sampling in a so-called stack-of-stars scheme allows detection of motion from a 1-dimensional projection of all signal in the head-feet direction (A). A compressed sensing reconstruction of all data in the expiration phase (periods in which the red curve is between the 2 dotted lines in A) provides a 3D image set in that phase, in which in 1 partition 3 healthy lymph nodes are visible as black dots (red arrows in B). Magnetic resonance imaging parameters: 3D T2*-weighted MRI with echo time 2.6 milliseconds (3 combined echoes), reconstructed resolution $1.15 \times 1.15 \times 1.25$ mm, acquisition time 4 minutes.

nodes in the upper abdomen can be attained (Fig. 4). In these radial pulse sequence schemes, motion of the abdomen is deducted from the continuously sampled MRI data itself, after which the breathing motion cycle is divided into multiple phases. The radially sampled k-space data from one phase within the cycle is combined into one 3D set of images using compressed sensing techniques. Choosing, for example, the expiration phase of breathing subsequently allows for reconstruction of a stationary image set of this particular breathing phase with high spatial resolution without blurring due to motion (Fig. 4).

NOTE THE NODES—THE CASE FOR HIGH-RESOLUTION 3D IMAGING

When discussing the clinical use of MRI for N-staging, some new concepts seem to appear, for example, MRI-guided histopathology.

Currently, when lymph node dissection specimens are evaluated by the pathologist to identify suspicious lymph nodes, the validation of the presence or absence of metastases can be challenging and laborious. The use of tactile sense to identify lymph nodes within a specimen is not always reliable, and fine slicing of the whole specimen can rapidly lead to enormous amounts of to-be-evaluated material, delaying the working process and causing rising costs. Using ex vivo MRI to scan the specimen as an intermediate step before the histopathological work-up can provide rapid and precise information about the amount, location, and also (if using USPIO enhancement before surgery) potentially the presence of metastases in the specimen. An ex vivo MRI of a resected specimen in a separate preclinical MR system allows annotation of individual lymph nodes in 3D scans with isotropic spatial resolution in the order of $0.3 \times 0.3 \times 0.3$ mm^3.[57] The annotated nodes, in relative position to anatomical landmarks like blood vessels, allow
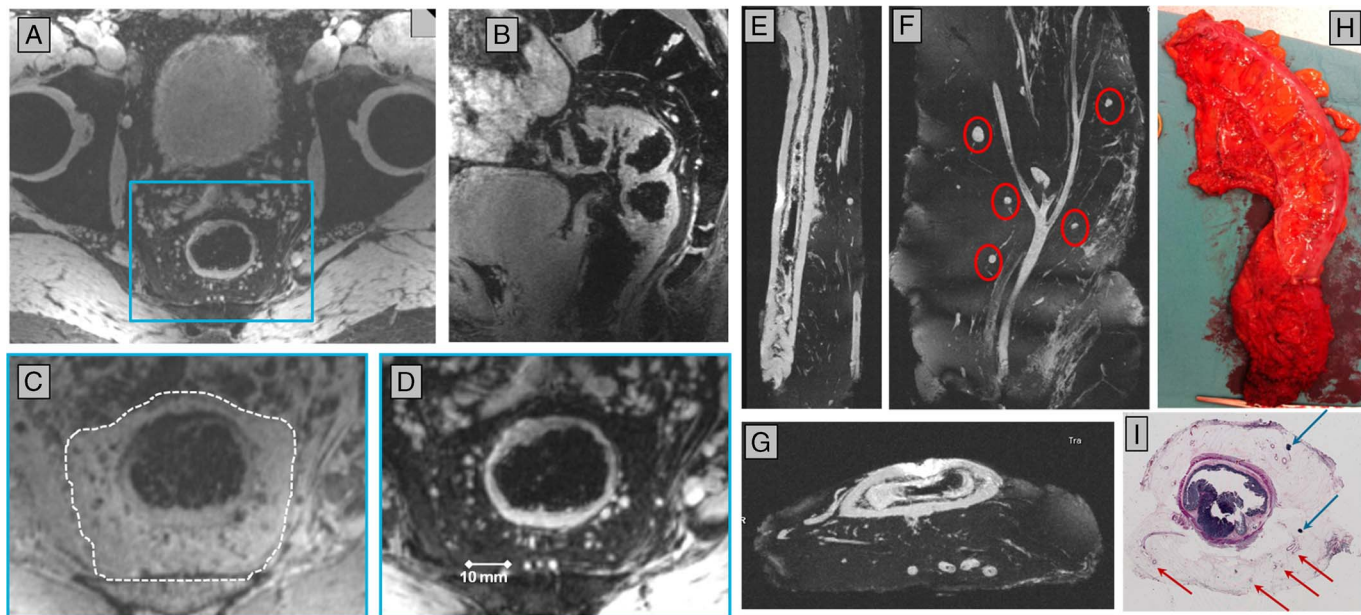

FIGURE 5. Node-to-node correlation of in vivo detected lymph nodes with histopathology. Before surgery, a patient with rectal cancer underwent 7 T MRI (A–D). Axial (A) and sagittal (B) reconstructions of a 3D MR image dataset with water excitation allowed identification of lymph nodes in the mesorectum. An inset (blue box in A) of the mesorectum (dotted line in C) is shown with lipid (C) or water (D) excitation. After surgery, an ex vivo MRI of water in the specimen (H) in a preclinical 7 T MR system provides high anatomical detail in 3 orientations (E–G) of lymph nodes (red circles in F) and blood vessels in the mesorectum. Vessels and nodes in relative position to the rectum serve as anatomical landmarks to register lymph nodes from in vivo to ex vivo MRI. With these ex vivo images available during histopathological work-up, annotated lymph nodes can be registered from in vivo MRI to histopathology (I).
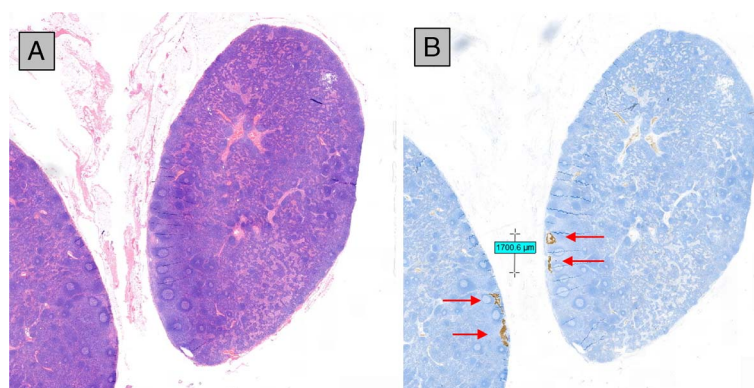
FIGURE 6. Hematoxylin and eosin staining (A) and immunohistochemistry (B) of 2 neighboring sections of a lymph node of an elective lymph node dissection of a patient with squamous cell carcinoma of the tongue with a clinically negative neck. Immunohistochemistry reveals a nodal micrometastasis (red arrows) with a long axis of 1.7 mm. This was 1 from 2 positive lymph nodes from a total of 24 resected nodes from 3 nodal stations. Cancer deposits of this size will be very challenging to pick up with current in vivo imaging methods.

cognitive registration to in vivo MR images. If these ex vivo 3D MRI scans are available when cutting the specimen for histopathological work-up, the annotation of the nodes can be copied to nodes harvested from the specimen, completing a node-to-node correlation of in vivo MRI with histopathology (Fig. 5). Although this workflow allows the identification of many (small) lymph nodes or lymph node–like structures on ex vivo MRI in, for example, rectal cancer specimens, it remains challenging to harvest all structures below 2 mm in size when slicing the large specimens. After multiple cuts, the exact registration between specimen and ex vivo MRI is lost, and then MRI-guided histopathology does not increase lymph node yield over standard pathological work-up anymore.[57] Smaller specimens, or a full 3D approach for histopathological reconstruction of larger specimens, could bring the numbers of ex vivo MRI-detected and histopathologically confirmed nodes closer together. The spatial resolution of ex vivo MRI is high enough to identify all nodes in the specimen. If individual nodes are harvested without the surrounding tissue, realignment of orientation of the nodes from in vivo to histopathology is a remaining challenge.

From a histopathological view, the presence of a macrometastasis (tumor deposit of ≥2 mm) or even micrometastases (tumor deposits between 0.2 and 2 mm) on 1 section of a node already makes the lymph node positive (Fig. 6). The in-plane resolution of standard hematoxylin and eosin histopathological sections can be less than a micron, whereas in the third dimension, the section represents 2 to 3 mm of the node (or a complete node). With 3D MRI, signal from the full node can be acquired with an isotropic resolution of less than 1 mm. These differences in nodal sampling need to be taken into account when comparing MRI with histopathology. If the aim of in vivo MRI is to detect macrometastases and perhaps also micrometastases, the highest attainable isotropic resolution with functional contrast between healthy and suspicious tissue is warranted. In young healthy volunteers, the number of lymph nodes detected in vivo in the pelvic area with MRI at 7 T showed a large variation, and 69% of a total of 564 lymph nodes were 2 mm or smaller.[58] This suggests that not only macrometastases but also micrometastases in the order of 1 mm can be visualized in vivo if proper functional imaging contrast to differentiate between healthy and suspicious nodal tissue is applied.

FUTURE OUTLOOK

Observing the newest developments described in this work, we expect an increasing role of MRI in nodal staging with further clinical implementation and scientific evaluation of USPIO-enhanced MRI. Further development and evaluation of new MRI pulse sequences are

very important to enable scanning in moving areas such as the upper abdomen and mediastinum. This would enable high-quality N-staging in tumor entities like esophageal or pancreatic cancer. Also, the possible quantification of MRI parameters in USPIO-enhanced MRI is of high interest—this is the first step for the development of automated reading algorithms using Artificial Intelligence for clinical reading. If realized, this would be a giant leap in broad implementation of these techniques into clinical practice. Finally, as mentioned above, the use of MRI in the clinical setting but not directly in-vivo (like in pathology) would make the N-staging assessment faster and more precise, resulting in generally better N-staging diagnostics. This also could have a tremendous impact on the management of oncologic patients.

CONCLUSION

The clinical need for more precise, reliable, and noninvasive N-staging in patients with solid tumors is evident. Using USPIO-enhanced MRI offers great diagnostic possibilities for N-staging of different types of cancer, including the 4 examples given in this work (head and neck cancer, esophageal cancer, rectal cancer, and prostate cancer). The MR visualization of (even small) lymph node metastases is the fundament for MR-guided therapy approaches, first of all MR-guided radiotherapy. The excellent soft tissue contrast of MRI and an USPIO-based differentiation of metastatic versus nonmetastatic lymph nodes could potentially enable more precise therapy and, therefore, fewer side effects, essentially in cancer patients in oligometastatic stage. Further scientific and clinical development is needed to assess the accuracy of USPIO-enhanced MRI of detecting small metastatic deposits for different cancer types in different anatomical locations and to broaden the indications for the use of (USPIO-enhanced) MRI in lymph node imaging in clinical practice.

REFERENCES

1. Psychogios G, Mantsopoulos K, Bohr C, et al. Incidence of occult cervical metastasis in head and neck carcinomas: development over time. *J Surg Oncol*. 2013; 107:384–387.
2. Alba JR, Basterra J, Ferrer JC, et al. Hypothyroidism in patients treated with radiotherapy for head and neck carcinoma: standardised long-term follow-up study. *J Laryngol Otol*. 2016;130:478–481.
3. Armanious MA, Mohammadi H, Khodor S, et al. Cardiovascular effects of radiation therapy. *Curr Probl Cancer*. 2018;42:433–442.
4. Gane EM, Michaleff ZA, Cottrell MA, et al. Prevalence, incidence, and risk factors for shoulder and neck dysfunction after neck dissection: a systematic review. *Eur J Surg Oncol*. 2017;43:1199–1218.
5. Strojan P, Hutcheson KA, Eisbruch A, et al. Treatment of late sequelae after radiotherapy for head and neck cancer. *Cancer Treat Rev*. 2017;59:79–92.

6. van Hagen P, Hulshof MC, van Lanschot JJ, et al. Preoperative chemoradiotherapy for esophageal or junctional cancer. *N Engl J Med*. 2012;366:2074–2084.

7. de Gouw DJJM, Klarenbeek BR, Driessen M, et al. Detecting pathological complete response in esophageal cancer after neoadjuvant therapy based on imaging techniques: a diagnostic systematic review and meta-analysis. *J Thorac Oncol*. 2019;14:1156–1171.

8. Little AG, Lerut AE, Harpole DH, et al. The Society of Thoracic Surgeons practice guidelines on the role of multimodality treatment for cancer of the esophagus and gastroesophageal junction. *Ann Thorac Surg*. 2014;98:1880–1885.

9. Ajani JA, D'Amico TA, Bentrem DJ, et al. Esophageal and esophagogastric junction cancers, version 2.2019, NCCN Clinical Practice Guidelines in Oncology. *J Natl Compr Canc Netw*. 2019;17:855–883.

10. Beets-Tan RGH, Lambregts DMJ, Maas M, et al. Magnetic resonance imaging for clinical management of rectal cancer: updated recommendations from the 2016 European Society of Gastrointestinal and Abdominal Radiology (ESGAR) consensus meeting. *Eur Radiol*. 2018;28:1465–1475.

11. Brouwer NPM, Stijns RCH, Lemmens V, et al. Clinical lymph node staging in colorectal cancer; a flip of the coin? *Eur J Surg Oncol*. 2018;44:1241–1246.

12. Elferink MAG, Siesling S, Lemmens VEPP, et al. Variation in lymph node evaluation in rectal cancer: a Dutch nationwide population-based study. *Ann Surg Oncol*. 2011;18:386–395.

13. Brouwer NPM, Bos ACRK, Lemmens VEPP, et al. An overview of 25 years of incidence, treatment and outcome of colorectal cancer patients. *Int J Cancer*. 2018;143:2758–2766.

14. Langman G, Patel A, Bowley DM. Size and distribution of lymph nodes in rectal cancer resection specimens. *Dis Colon Rectum*. 2015;58:406–414.

15. Wang C, Zhou Z, Wang Z, et al. Patterns of neoplastic foci and lymph node micrometastasis within the mesorectum. *Langenbecks Arch Surg*. 2005;390:312–318.

16. Allen SD, Padhani AR, Dzik-Jurasz AS, et al. Rectal carcinoma: MRI with histologic correlation before and after chemoradiation therapy. *AJR Am J Roentgenol*. 2007;188:442–451.

17. Pierredon-Foulongne MA, Nougaret S, Bibeau F, et al. Utility of reassessment after neoadjuvant therapy and difficulties in interpretation. *Diagn Interv Imaging*. 2014;95:495–503.

18. Mottet N, Bellmunt J, Bolla M, et al. EAU-ESTRO-SIOG guidelines on prostate cancer, part 1: screening, diagnosis, and local treatment with curative intent. *Eur Urol*. 2017;71:618–629.

19. Fossati N, Willemse PM, van den Bergh T, et al. The benefits and harms of different extents of lymph node dissection during radical prostatectomy for prostate cancer: a systematic review. *Eur Urol*. 2017;72:84–109.

20. Heesakkers RAM, Jager GJ, Hövels AM, et al. Prostate cancer: detection of lymph node metastases outside the routine surgical area with ferumoxtran-10-enhanced MR imaging. *Radiology*. 2009;251:408–414.

21. Joniau S, Van den Bergh L, Lerut E, et al. Mapping of pelvic lymph node metastases in prostate cancer. *Eur Urol*. 2013;63:450–458.

22. Larbi A, Dallaudière B, Pasoglou V, et al. Whole body MRI (WB-MRI) assessment of metastatic spread in prostate cancer: therapeutic perspectives on targeted management of oligometastatic disease. *Prostate*. 2016;76:1024–1033.

23. Bravi CA, Fossati N, Gandaglia G, et al. Assessing the best surgical template at salvage pelvic lymph node dissection for nodal recurrence of prostate cancer after radical prostatectomy: when can bilateral dissection be omitted? Results from a multi-institutional series. *Eur Urol*. 2020.

24. Hövels AM, Heesakkers RA, Adang EM, et al. The diagnostic accuracy of CT and MRI in the staging of pelvic lymph nodes in patients with prostate cancer: a meta-analysis. *Clin Radiol*. 2008;63:387–395.

25. Vos EK, Kobus T, Litjens GJ, et al. Multiparametric magnetic resonance imaging for discriminating low-grade from high-grade prostate cancer. *Invest Radiol*. 2015;50:490–497.

26. Maas MC, Litjens GJS, Wright AJ, et al. A single-arm, multicenter validation study of prostate cancer localization and aggressiveness with a quantitative multiparametric magnetic resonance imaging approach. *Invest Radiol*. 2019;54:437–447.

27. Muteganya R, Goldman S, Aoun F, et al. Current imaging techniques for lymph node staging in prostate cancer: a review. *Front Surg*. 2018;5:74.

28. Dadfar SM, Roemhild K, Drude NI, et al. Iron oxide nanoparticles: diagnostic, therapeutic and theranostic applications. *Adv Drug Deliv Rev*. 2019;138:302–325.

29. Turkbey B, Czarniecki M, Shih JH, et al. Ferumoxytol-enhanced MR lymphography for detection of metastatic lymph nodes in genitourinary malignancies: a prospective study. *AJR Am J Roentgenol*. 2020;214:105–113.

30. US Food and Drug Administration. FDA Drug Safety Communication: FDA strengthens warnings and changes prescribing instructions to decrease the risk of serious allergic reactions with anemia drug Feraheme (ferumoxytol). March 3, 2016. Available at: www.fda.gov/drugs/drug-safety-and-availability/fda-drug-safety-communication-fda-strengthens-warnings-and-changes-prescribing-instructions-decrease. Accessed October 23, 2020.

31. Elhalawani H, Awan MJ, Ding Y, et al. Data from a terminated study on iron oxide nanoparticle magnetic resonance imaging for head and neck tumors. *Sci Data*. 2020;7:63.

32. Fortuin AS, Bruggemann R, van der Linden J, et al. Ultra-small superparamagnetic iron oxides for metastatic lymph node detection: back on the block. *Wiley Interdisc Rev Nanomed Nanobiotechnol*. 2018;10:e1471.

33. Harisinghani MG, Barentsz J, Hahn PF, et al. Noninvasive detection of clinically occult lymph-node metastases in prostate cancer. *N Engl J Med*. 2003;348:2491–2499.

34. Heesakkers RAM, Hövels AM, Jager GJ, et al. MRI with a lymph-node-specific contrast agent as an alternative to CT scan and lymph-node dissection in patients with prostate cancer: a prospective multicohort study. *Lancet Oncol*. 2008;9:850–856.

35. Wu L, Cao Y, Liao C, et al. Diagnostic performance of USPIO-enhanced MRI for lymph-node metastases in different body regions: a meta-analysis. *Eur J Radiol*. 2011;80:582–589.

36. DeMarzo AM, Nelson WG, Isaacs WB, et al. Pathological and molecular aspects of prostate cancer. *Lancet*. 2003;361:955–964.

37. Ghosh A, Heston WDW. Tumor target prostate specific membrane antigen (PSMA) and its regulation in prostate cancer. *J Cell Biochem*. 2004;91:528–539.

38. Perera M, Papa N, Roberts M, et al. Gallium-68 prostate-specific membrane antigen positron emission tomography in advanced prostate cancer-updated diagnostic utility, sensitivity, specificity, and distribution of prostate-specific membrane antigen-avid lesions: a systematic review and meta-analysis. *Eur Urol*. 2020;77:403–417.

39. Hofman MS, Lawrentschuk N, Francis RJ, et al. Prostate-specific membrane antigen PET-CT in patients with high-risk prostate cancer before curative-intent surgery or radiotherapy (proPSMA): a prospective, randomised, multicentre study. *Lancet*. 2020;395:1208–1216.

40. van Kalmthout LWM, van Melick HHE, Lavalaye J, et al. Prospective validation of gallium-68 prostate specific membrane antigen-positron emission tomography/computerized tomography for primary staging of prostate cancer. *J Urol*. 2020;203:537–545.

41. Jansen BHE, Bodar YJL, Zwezerijnen GJC, et al. Pelvic lymph-node staging with ^{18}F-DCFPyL PET/CT prior to extended pelvic lymph-node dissection in primary prostate cancer—the SALT trial [published online ahead of print August 12, 2020]. *Eur J Nucl Med Mol Imaging*.

42. Klingenberg S, Jochumsen MR, Ulhøi BP, et al. (68)Ga-PSMA PET/CT for primary NM staging of high-risk prostate cancer [published online ahead of print May 22, 2020]. *J Nucl Med*. jnumed.120.245605.

43. Winkel D, Werensteijn-Honingh AM, Eppinga WSC, et al. Dosimetric feasibility of hypofractionation for SBRT treatment of lymph node oligometastases on the 1.5T MR-linac [published online ahead of print September 16, 2020]. *Radiother Oncol*.

44. Foster CC, Weichselbaum RR, Pitroda SP. Oligometastatic prostate cancer: reality or figment of imagination? *Cancer*. 2019;125:340–352.

45. Fraser M, Koontz B, Emmenegger U, et al. What is Oligometastatic prostate cancer? *Eur Urol Focus*. 2019;5:159–161.

46. Tosoian JJ, Gorin MA, Ross AE, et al. Oligometastatic prostate cancer: definitions, clinical outcomes, and treatment considerations. *Nat Rev Urol*. 2017;14:15–25.

47. Heesakkers RAM, Fütterer JJ, Hövels AM, et al. Prostate cancer evaluated with ferumoxtran-10-enhanced T2*-weighted MR imaging at 1.5 and 3.0 T: early experience. *Radiology*. 2006;239:481–487.

48. Orzada S, Maderwald S, Poser BA, et al. RF excitation using time interleaved acquisition of modes (TIAMO) to address B1 inhomogeneity in high-field MRI. *Magn Reson Med*. 2010;64:327–333.

49. Rietsch SHG, Orzada S, Maderwald S, et al. 7T ultra-high field body MR imaging with an 8-channel transmit/32-channel receive radiofrequency coil array. *Med Phys*. 2018;45:2978–2990.

50. Philips BWJ, Fortuin AS, Orzada S, et al. High resolution MR imaging of pelvic lymph nodes at 7 tesla. *Magn Reson Med*. 2017;78:1020–1028.

51. Philips BWJ, Stijns RCH, Rietsch SHG, et al. USPIO-enhanced MRI of pelvic lymph nodes at 7-T: preliminary experience. *Eur Radiol*. 2019;29:6529–6538.

52. Giovagnoni A, Valeri G, Ferrara C. MRI of esophageal cancer. *Abdom Imaging*. 2002;27:361–366.

53. de Gouw DJJM, Maas MC, Slagt C, et al. Controlled mechanical ventilation to detect regional lymph node metastases in esophageal cancer using USPIO-enhanced MRI; comparison of image quality [published online ahead of print September 20, 2020]. *Magn Reson Imaging*. S0730-725X(20)30336-2 https://doi.org/10.1016/j.mri.2020.09.020.

54. Chandarana H, Feng L, Block TK, et al. Free-breathing contrast-enhanced multiphase MRI of the liver using a combination of compressed sensing, parallel imaging, and golden-angle radial sampling. *Invest Radiol*. 2013;48:10–16.

55. Feng L, Axel L, Chandarana H, et al. XD-GRASP: golden-angle radial MRI with reconstruction of extra motion-state dimensions using compressed sensing. *Magn Reson Med*. 2016;75:775–788.

56. Feng L, Grimm R, Block KT, et al. Golden-angle radial sparse parallel MRI: combination of compressed sensing, parallel imaging, and golden-angle radial sampling for fast and flexible dynamic volumetric MRI. *Magn Reson Med*. 2014;72:707–717.

57. Stijns R, Philips B, Wauters C, et al. Can ex vivo magnetic resonance imaging of rectal cancer specimens improve the mesorectal lymph node yield for pathological examination? *Invest Radiol*. 2019;54:645–652.

58. Fortuin AS, Philips BWJ, van der Leest MMG, et al. Magnetic resonance imaging at ultra-high magnetic field strength: an in vivo assessment of number, size and distribution of pelvic lymph nodes. *PLoS One*. 2020;15:e0236884.